Friction
https://doi.org/10.1007/s40544-024-0940-1
ISSN 2223-7690
CN 10-1237/TH
RESEARCH ARTICLE

Fabrication of PMMA nanocomposite biomaterials reinforced by cellulose nanocrystals extracted from rice husk for dental applications

Ahmed FOULY[1,2,3,*], Walid M. DAOUSH[2,4,5], Hesham I. ELQADY[6], Hany S. ABDO[7,8]

[1] *Mechanical Engineering Department, College of Engineering, King Saud University, Riyadh 11421, Saudi Arabia*

[2] *The King Salman Center for Disability Research, Riyadh 11421, Saudi Arabia*

[3] *Department of Production Engineering and Mechanical Design, Faculty of Engineering, Minia University, Minia 61519, Egypt*

[4] *Department of Chemistry, College of Science, Imam Mohammad Ibn Saud Islamic University (IMSIU), Riyadh 11623, Saudi Arabia*

[5] *Faculty of Technology and Education, Helwan University, Cairo 11281, Egypt*

[6] *Faculty of Engineering, Aswan University, Aswan 81528, Egypt*

[7] *Center of Excellence for Research in Engineering Materials (CEREM), King Saud University, Riyadh 11421, Saudi Arabia*

[8] *Mechanical Design and Materials Department, Faculty of Energy Engineering, Aswan University, Aswan 81521, Egypt*

Received: 16 March 2024 / Revised: 02 May 2024 / Accepted: 29 May 2024

Abstract: The primary objective of global studies is to develop the properties and durability of polymers for various applications. When it comes to dental disability, denture base materials must have sufficient mechanical and tribological performance in order to withstand the forces experienced in the mouth. This work aims to investigate the effects of the addition of low content of cellulose nanocrystals (CNC) on the mechanical and tribological performance of the polymethyl methacrylate (PMMA) nanocomposites. Different weight percent of CNC (0, 0.2, 0.4, 0.6, and 0.8 wt%) were added to the PMMA matrix followed by ball milling to evenly distribute the nanoparticles reinforced phase in the matrix phase. The findings emphasize the significant impact of CNC integration on the performance of PMMA nanocomposites. By increasing the content of the CNC nanoparticles, the mechanical properties of PMMA were improved. In addition, the tribological outcomes demonstrated a significant reduction in the friction coefficient besides an enhancement in the wear resistance as the weight percentage of nanoparticles increased. The surface of the worn samples was investigated by utilizing SEM to identify the wear mechanisms corresponding to the different compositions. In addition, a finite elment model (FEM) was developed to ascertain the thickness of the worn layer and the generated stressed on the surfaces of the nanocomposite throughout the friction process.

Keywords: polymethyl methacrylate nanocomposite; cellulose nanocrystals; denture materials; rice husk; polymethyl methacrylate (PMMA); wear resistance

1 Introduction

Dentures must have appropriate mechanical and tribological characteristics in order to withstand against the different abrasion and friction forces that occur in the oral cavity [1]. In addition, the polymeric materials must possess biocompatibility and prevent any chemical interactions that may pose possible toxicity to the human bodies. Polymethyl methacrylate (PMMA) has been extensively utilized in denture production since 1937. The utilization of PMMA returns to its low weight, pleasing appearance, simplicity of manipulation and polishing, ability to be used in medical procedures, cost efficiency, and

* Corresponding author: Ahmed FOULY, E-mail: Amohammed7.c@ksu.edu.sa

ability to remain stable in the mouth [2]. The various advantages of PMMA encourage dentists utilizing it as a base material for denture and dental restorative polymers for many years. Conventionally, dentures are fabricated by combining pre-polymerized PMMA powder with liquid methyl methacrylate (MMA) monomers, and the resulting paste is then poured into dental molds.

However, PMMA may not always be the most suitable option for these applications. Due to its weak surface qualities, this material is not suited for applications that involve friction. Additionally, its mechanical properties, including flexural and impact strengths, are insufficient [3]. When used as a material for denture bases, PMMA experiences many types of stresses, including compressive, tensile, and shear stresses, which may cause scratches and fractures, and enhance wear rate. This has the capacity to modify the shape of the denture base, which presents a possible hazard to the patient welfare [4]. Significantly, abrupt fractures frequently occur as a result of the low resilience and fragility of pure PMMA, leading to inconvenience for patients and rise the overall expenses and treatment time. Harrison et al. [5] conducted a statistical analysis that defined the observed forms of fractures in denture bases composed of PMMA. It was observed that 29% of breakage was observed in fully intact upper dentures, while a further 38% of the other breakage appeared in the above partial dentures PMMA connectors.

The major criteria for selecting materials used for denture are to consist of sufficient strength, hardness, and resistance to erosion [6]. In order to deal with the PMMA qualities limit, many efforts are engaged to improve its performance through different modifications. Plasma technology has been used to make chemical alterations that enhance impact resistance. Additionally, researchers have investigated the use of cross-linking agents [7]. Furthermore, there have been efforts to strengthen PMMA by combination with various additive materials, such as reinforcing fillers (particles and fibers) which typically improve the polymer composite properties [8]. Kanie et al. [9] reported that the incorporation of fillers is widely acknowledged as a highly effective approach to enhance the different properties of composites. Turkyilmaz et al. [10] studied the influence of the addition of several additives of metal oxides (TiO_2, ZrO_2, and Al_2O_3) to the PMMA resin. The study revealed improvements in the PMMA properties such as fracture toughness. Nevertheless, the combination of these constituents had certain medically unfavorable consequences when coming into contact with saliva. The results obtained from investigating the combinations of ZrO_2/Al_2O_3 and ZrO_2/TiO_2 [11] were in line with the findings of Asar et al. [10]. In a similar manner, Akil et al. [12] examined the hardness, toughness, and strength of PMMA by the addition of various additives, such as nitrile butadiene rubber and ceramic additives like Al_2O_3 and yttria stabilized zirconia (YSZ), along with a silane agent. The mechanical performance has been enhanced, and the best combination has been determined to consist of 2.5% YSZ, 2.5% Al_2O_3, and 7.5% NBR. It is worth to mention that the samples weight of pure PMMA and its composite varied greatly because of the substantial amount of fillers, particularly the ceramic ones.

Nanotechnology has recently achieved substantial advancements in the field of material science which has the great effect on the material properties due to its unique properties comparing with its corresponding bulk materials. As a result, scientists have endeavored to integrate nanotechnology into the field of dentistry. The properties of nanocomposites depend on various aspects, including the dimensions, composition, structure, distribution, and weight fraction of the nano additives [13–15]. Nodehi et al. [16] examined the impact of double-modified nano-clays (organic filler) on the properties of PMMA used as a base for denture. Incorporating 0.5 wt% of clay nanoparticles fillers led to a significant enhancement of 32% in fracture toughness, 30% in flexural strength, and 65.8% in flexural modulus. Salahuddin [17] investigated the effect of weight fraction and shape of ZnO nanoparticles on the thermomechanical properties of the PMMA/ZnO nanocomposites. The study recorded a notable increase in the ability to withstand force with the utilization of ZnO nanotubes. On the other hand, the inclusion of ZnO nanospheres improved the ability to resist the bending forces. Researchers looked into the tribomechanical behavior of PMMA that had nano-titania and calcium aluminate added to it in different concentrations (1 to 5 vol%) and used both theory and experimental methods [18].

Rashed et al. [19] study the evaluation of the frictional performance of PMMA nanocomposites by the addition of hybrid nanomaterials such as graphene, SiO_2, and TiO_2. When the oxide nanoparticles content was increased, the results showed a significant rise in wear resistance. The study also found that as the filler volume fraction increased, the Young's modulus, toughness, hardness, and compression strength all got better over time. It's worth to mention that the tribological characteristics such as wear resistance and coefficient of friction are improved. Huang et al. [20] study the strengthening of PMMA by including various amounts of carbon nanotubes (CNTs), which led to a significant decrease in its friction coefficient and an enhancement in its resistance to abrasion. Nevertheless, the extensive utilization of CNTs is mostly constrained by aesthetic factors. Another investigation is performed by Ablawa et al. [21], various proportions of TiO_2/ZnO nanoparticles (NP) additives were added to PMMA, resulting in a decrease in both wear and coefficient of friction as the NP content and sliding period increased. Ali et al. [22] enhanced the strength of both cold- and hot-cured PMMA by using multi-walled carbon nanotubes (MWCNTs). The hot-cured resin exhibited good wear resistance and hardness as the loading of MWCNT increased to 0.3 wt%. Moreover, there was a significant reduction in the coefficient of friction for both cold- and hot-cured PMMA.

Cellulose, the predominant organic biopolymer in nature, is abundant in various sources such as cysts, wood, algae, bacteria, and plants. It exhibits various shapes and possesses advantageous properties, such as a high elasticity, excellent crystallinity, and a large aspect ratio. Hence, nanocellulose compounds are extensively utilized in several industries including textiles, paper-making, medicines, and cosmetics [23–26]. Manmade nanocellulose could be categorized into two primary categories: cellulose nanofibers (CNFs) and cellulose nanocrystals (CNCs). Both types include the utilization of a traditional cellulose extraction method to remove non-cellulose components from the original lignocellulosic material. Commonly, carbon nanofibers (CNFs) are produced by high-energy mechanical techniques like ultrasonic vibration, high-pressure homogenization, and grinding [27, 28]. Both CNFs and CNCs, extracted from sources such as rice straws, are natural polymer materials that possess non-toxic properties, as well as high specific strength and stiffness. Consequently, they are highly effective components in the fabrications of composites, specifically in eco-friendly biopolymer composites. Alhavaz et al. [29] investigated the application of nanocrystalline cellulose as a strengthening additive for dental materials. The study examined the strength and hardness of PMMA, in which the nanocrystalline cellulose was added at different concentrations ranging from 1 to 5 wt%. The inclusion of nanocrystalline cellulose by 2.5 wt% led to the enhancement in Vickers hardness by 13% and strength by 16%. In addition, the incorporation of cellulose and hydroxyapatite in a 50% proportion enhanced its mechanical performance; for example, hardness, compressive strength, and flexural strength/modulus [30]. This enhancement in the properties indicates nanocrystalline cellulose appropriateness as additive for dental restorative materials. Nevertheless, it is important to acknowledge that employing nanomaterials at elevated loading ratios can result in increased expenses. Consequently, researchers suggests using nanopartricles additives in a suitable content, particularly at low weight fractions below 1 wt% [31].

The major purpose of this study is to examine how adding small amounts (0 to 0.8 wt%) of cellulose nanocrystals (CNCs) affects the mechanical and tribological behavior of PMMA. A comprehensive manufacturing method for CNCs derived from rice husk is carried out. The mechanical properties, including hardness, relative toughness, elongation, yield strength, and the elasticity, are investigated. The proposed nanocomposites are rubbed on a disk made of stainless steel as part of the tribological testing. In order to deep understand the experimental results, an FEM is created to examine the contact stresses produced throughout the tribological tests. The current study utilizes a comprehensive methodology, including experimental tests and finite element analysis to precisely assess the impact of CNCs on PMMA. In addition, the cellulose nanocrystals, nanocomposites, besides the surfaces tested for friction are analyzed using XRD and SEM to evaluate their morphological and structural characteristics.

Consequently, the effects of low concentrations of CNCs on both the mechanical behavior, wear properties, and wear mechanism of PMMA are performed.

2 Materials and methods

2.1 Materials and fabrication process

This investigation utilized self-curing acrylic resin that was obtained from a Spanish company Protechno Famadent S.L.U. Denture plates made of acrylic can be repaired and relined with the help of this tailored resin. The resin is ideal for dental applications since it cures naturally, without the use of heat or other curing agents. Both partial and full dentures can be hydro-flasked. The package comes in two components: a white PMMA powder with a 1.18 g/cm^3 density, serving as the main polymer, and a transparent MMA liquid with a 0.94 g/cm^3 density, acting as the monomer.

On the other hand, the initial step in the extraction process of the cellulose nanocrystals involved subjecting the rice husk (RH) to a comprehensive washing regimen. Specifically, the husk underwent a meticulous series of 2–4 washes with distilled water. This rigorous washing procedure was designed to effectively eliminate impurities and water-soluble substances adhering to the rice husk fibers. Subsequently, the washed RH was undergoing air-drying for a duration of more than 12 h to ensure the removal of any residual moisture. Moving on to the extraction of cellulose nanocrystals (CNC), a multi-step protocol was followed. Firstly, an alkali treatment was employed to eradicate lignin and hemicellulose from the RH fibers. This involved the utilization of 30% sodium hydroxide with a carefully measured raw material to liquor ratio of 1:10. The mixture underwent mechanical stirring for a duration of 4 h by boiling at a temperature of 100 °C. This alkali treatment was repeated twice to enhance the effectiveness of the process. After the treatment, the obtained material was subjected to washing with distilled water, followed by air-drying at 50 °C for an additional 12 h. In the subsequent phase, a bleaching process was introduced into the extraction procedure. This entailed the use of 2% hydrogen peroxide (H_2O_2) with a material-to-liquor ratio of 1:30, conducted at a pH value of 9. The bleaching operation involved mechanical stirring for 4 h at 80°C. Following the bleaching process, the material underwent repeated washing with distilled water using a vacuum pump, and further purification was achieved through Buchner filtration. The final step in this phase involved drying the material at 50 °C for 12 h in an air-reverberatory furnace. The next step in the extraction process involved acid hydrolysis, conducted at a temperature of 45 °C. A 64% (w/w) solution of sulphuric acid (H_2SO_4) was pre-heated for 40 minutes under continuous stirring. The hydrolyzed substance was subsequently washed and separated through a centrifugation process at 10,000 rpm and 10 °C for 10 min. It is noteworthy that this centrifugation step was iterated 10 times to ensure thorough separation. Following this, the resulting suspension underwent a prolonged dialysis process against distilled water over several days, aimed at achieving a consistent pH within the range of 5–6. The obtained suspension was then subjected to sonication at 40 kHz for a duration of 30 minutes before being refrigerated to arrest the reaction for subsequent utilization. Figure 1 illustrates a schematic for the CNC production process.

In order to produce the nanocomposite specimens, the calculated amounts of the PMMA and CNCs powders were weighed to achieve certain weight ratios ranged from 0 up to 0.8 wt% of CNCs with a step of 0.2 wt%. Afterward, the mixed powders were milling together using a ball milling machine for 10 minutes to ensure that the CNCs were evenly distributed into the PMMA raw material. Subsequently, the MA liquid monomer was introduced at varying weight ratios of solid to liquid, spanning from 5 to 3.5. The weight of the final solid powder was obtained by adding together the weights of the PMMA and CNCs powders. Subsequently, the ball milled powder and the MMA were blended manually at 30 °C and 35% relative humidity. After attaining a viscous and malleable texture, which usually takes approximately 20–30 s of mixing process, the viscus liquid was molded into a cylindrical die of 25 mm in height and 8 mm in diameter. It was then compressed

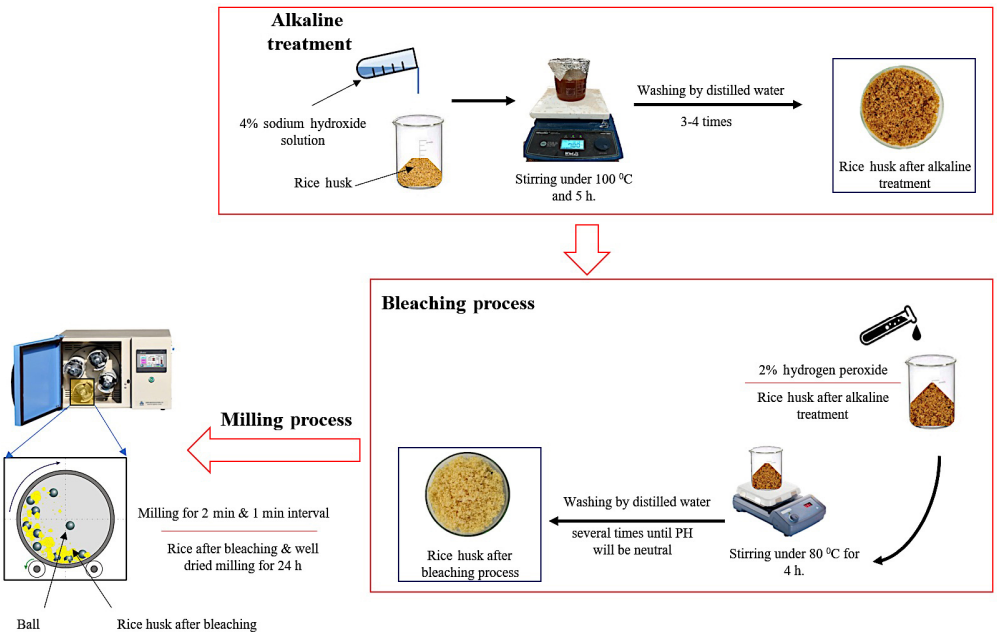

Fig. 1 Schematic flowchart of the CNC fabrication process.

using a pressure of 15 MPa. After the duration of 1 h, the obtained consolidated nanocomposites underwent complete solidification and were subsequently removed from the molds. The process was conducted following the guidelines and instructions provided by the PMMA manufacturer. The PMMA/CNCs samples with different weight fractions of CNCs 0, 0.2, 0.4, 0.6, and 0.8 wt% were represented as CNC_0, CNC_2, CNC_4, CNC_6, and CNC_8, respectively. Figure 2 illustrates a schematic flowchart of the fabrication process of the nanocomposite samples.

2.2 Testing and characterization

Diverse methods were employed to evaluate the chemical, physical, mechanical, and tribological characteristics of PMMA/CNCs nanocomposite samples. The chemical compositions in the current investigation of the CNCs and PMMA were analyzed using XRD technique. Furthermore, XRD was utilized to analyze the chemical composition of the PMMA/CNCs nanocomposites. Regarding the CNCs powder extracted from rice husk, FTIR and TGA were utilized to identify and confirm the chemical structure and characteristics of the prepared CNCs. In addition, SEM was employed to identify the morphology of the extracted CNCs.

The experimental measurement of the densities of PMMA/CNCs nanocomposites was conducted using Archimedes' principle [32]. The PMMA/CNCs nanocomposite samples weight was measured in both

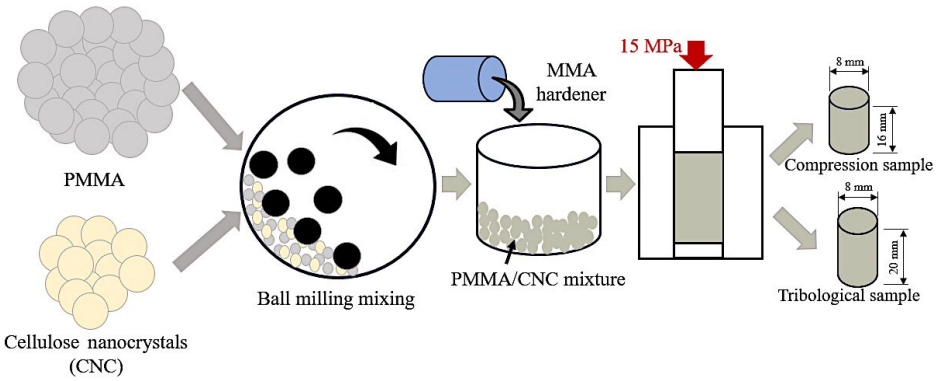

Fig. 2 Schematic flowcharts of PMMA/CNC nanocomposite production process.

air and alcohol as a floating fluids. Subsequently, the density was then calculated by using Eq. (1):

$$\rho_{\mathrm{PMMA/CNCs}} = \left(\rho_{\mathrm{alc}} + \rho_{\mathrm{air}}\right) \times \frac{m_{\mathrm{s-air}}}{m_{\mathrm{s-air}} - m_{\mathrm{s-alc}}} + \rho_{\mathrm{air}} \quad (1)$$

where $\rho_{\mathrm{PMMA/CNCs}}$ is the measured densities of the PMMA/CNCs nanocomposites in g/cm^3, ρ_{alc} is the density of the alcohol in g/cm^3, ρ_{air} is the density of air in g/cm^3, $m_{\mathrm{s-alc}}$ and $m_{\mathrm{s-air}}$ are the PMMA/CNCs nanocomposites masses in grams, in alcohol and in air, respectively.

The nanocomposite densities were determined 5 times for each corresponding nanocomposite specimen and the average value was estimated to ensure accuracy and reliability of the experimental results.

In order to evaluate the mechanical characteristics of PMMA nanocomposites containing small weight fractions of cellulose nanocrystals, cylindrical samples of 8 mm in diameter and 16 mm in length were fabricated according to the guidelines of the standard ISO 604 Plastics [33]. The hardness of the PMMA/CNCs nanocomposites was measured by applying a measured load of 5 ± 0.5 kg using tester of the model shore D durometer working in a dwell period of 15 s, according to the standards ASTM D2240 [34]. Hardness measurements were performed five times at various points on the nanocomposite surface; then, the mean value was determined. Subsequently, an Instron 5582 Microtester, a computer-controlled servo-hydraulic universal testing machine (Instron, University Ave, Norwood, USA), was used to conduct the compression tests. The stress–strain curves acquired from these experiments facilitated the extraction of crucial mechanical parameters, such as the elongation, toughness, yield strength, and elasticity. The mean values for all measured properties for each corresponding nanocomposite were calculated using experimental measurements by considering standard deviation.

The friction and wear behavior of PMMA/CNC nanocomposites were assessed in a controlled environment with no lubrication conditions at 28 °C temperature and 55% humidity. This was done employing a pin-on-disk reciprocating tribometer, stroke of 25-mm, according to the ASTM G99-95 standards guidelines [35], as displayed in Fig. 3. The PMMA/CNC samples serve as the pin of the tribometer and were fabricated with dimensions 8 mm in diameter and 20 mm in length. The tribometer pen, PMMA/CNC nanocomposite sample, was in contact with a rectangular stainless-steel disc and underwent sliding motion. The objective of this experiment was to replicate real-life situations in which PMMA is utilized as restorative material in dental, imitating the rubbing that occurs against PMMA in various teeth inside the mouth [36]. In addition, the study specifically investigated the tribological behavior that occurs when PMMA nanocomposites contact with steel equivalents. This research was prompted by cases when parents utilize crowns made of stainless steel to protect teeth of their children from being decay [37]. The stainless-steel disc exhibited a surface roughness of 0.025. Prior to each experiment, the disk surface was cleansed utilizing acetone and to ensure nothing of the acetone still in the surface, the surface was dried using a heat gun to eradicate remaining adhered contaminants. In addition, PMMA/CNC nanocomposite samples

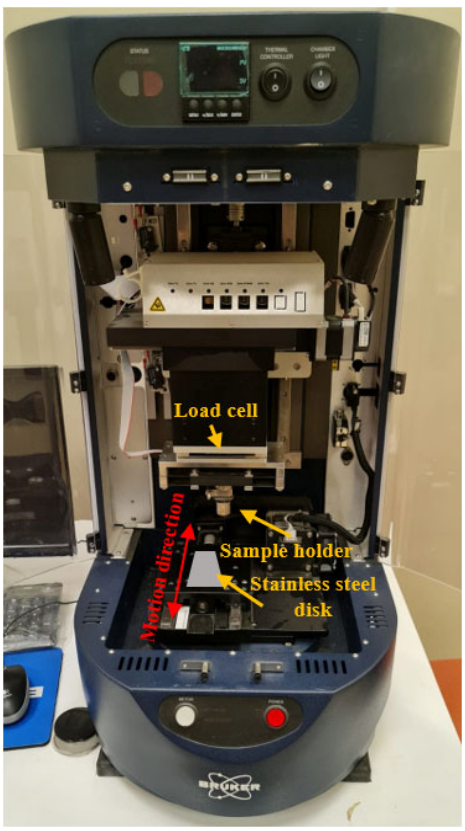

Fig. 3 Reciprocating tribometer.

underwent ultrasonic washing at 40 kHz and drying before testing. A steady 0.4 m/s frictional speed was used throughout the tribological testing, and a range of normal loads were applied, 2, 4, 6, 8, and 10 N. Wear was determined by assessing the variance in nanocomposites specimen weight before the frictional test and after finishing the experiment. To ensure accuracy and reliability, each frictional test was repeated 5 times under the same conditions. Subsequently, mean values and standard deviations were computed for a comprehensive analysis of the results. Following the completion of frictional tests, the morphology of the surfaces that were rubbed was analyzed using SEM microscope of model JCM-6000Plus, JEOL, Japan. The surface of each sample was coated by sputtering with a tiny layer of platinum prior to scanning in order to improve its conductivity.

3 Results and discussion

3.1 CNC and PMMA/CNC nanocomposites investigations

XRD technique was utilized to identify the crystalline behavior of the cellulose fibers which were isolated from the RH. The XRD data, as depicted in Fig. 4, vividly illustrates the crystalline structure of the CNC. This crystalline structure is attributed to the hydrogen bonding interactions between CNC molecules, resulting in a highly crystalline configuration, aligning with findings in Ref. [38]. The discernible impact of the chemical treatment applied to the natural RH is evident in the XRD results, indicating a notable influence on the crystallinity of the produced CNC. The observed narrow peaks in the diffractive pattern of CNC signify a rise in crystallinity of the cellulose fibers. This enhancement in crystallinity is expected correlated with the high stiffness and rigidity in the extracted CNC, subsequently contributing to its overall strength. A distinctive characteristic diffraction peak is identified at 2θ of 22°, corresponding to the (100) crystalline plane orientation. The intensity scattered by the amorphous component exhibits the lowest intensity at a diffraction angle of around 2θ of 19°. This nuanced XRD analysis provides a comprehensive understanding of the crystalline properties and structural characteristics of the prepared cellulose nanocrystals.

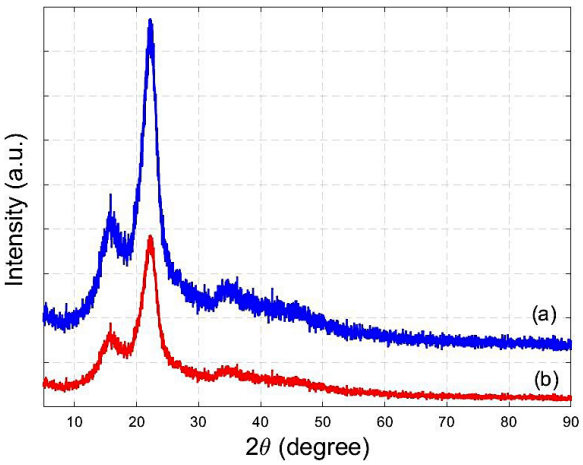

Fig. 4 XRD for (a) cellulose [38], and (b) the prepared CNC.

The prepared CNC extracted from the RH was investigated by FTIR. Figure 5 reveals consecutive discernible peaks that provide insights into the molecular composition. Notably, these peaks highlight the presence of the C–H bonding and hydroxyl O–H group within the CNC structure. Peaks at 1,639 and 3,436 cm^{-1} are corresponding to the characteristic vibrations of C–H and O–H groups, respectively. The presence of additional peaks, such as those at 1,639 and 3,436 cm^{-1}, may be due to the presence of the H–O–H hydrogen bonding with water of the moister content of the CNC remained from the extraction process. This can be attributed to residual cellulose components that may not have been completely isolated during the chemical treatment and the bleaching processes which applied to the sample. These peaks contribute to a more comprehensive understanding of the water absorption characteristics associated with the CNC extracted from the original rice husk. Furthermore, specific peaks at 1,037 and 825 cm^{-1} provide valuable information about the CNC structure. These peaks are indicative of the C–H stretching and vibration of C–O bonding, offering insights into the cellulose component's structural arrangement.

The TGA of the extracted CNC, depicted in Fig. 6, unveils a distinctive weight loss pattern primarily occurring below 100 °C. During this phase, the principal change is attributed to the loss of the water content by vaporization, a consequence of the

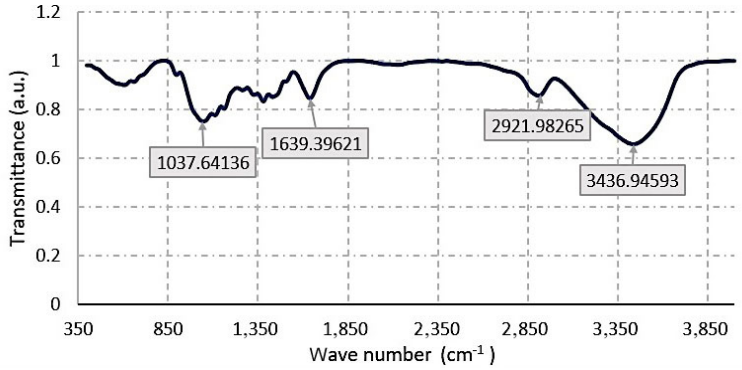

Fig. 5 FTIR spectrum of the prepared CNC.

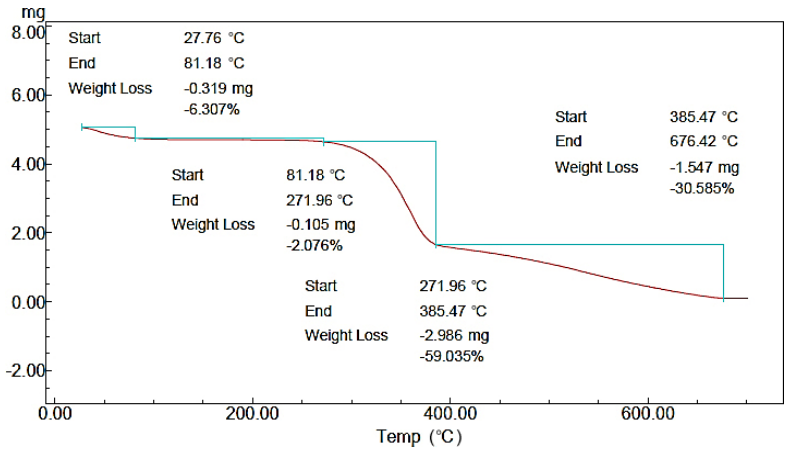

Fig. 6 TGA of the prepared CNC.

hydrophilic nature inherent to lignocellulose fibers. Notably, the extent of weight loss is directly linked to the initial humidity ratio of the produced CNC. By rising the temperature, specially starting from 254 °C, the weight losses escalate to 64%. This observed increase in weight loss indicates a decrease in the thermal stability of the induced CNC. This reduction in stability is attributed to the presence of hemicellulose, lignin, and pectin in the chemical composition, which contribute to the evolving weight loss characteristics. Beyond 400 °C, the weight losses in the material become more pronounced, primarily due to the presence of carbon content within the fibers' cellular structure. This detailed analysis of the TGA data provides a complete understanding of the thermal degradation behavior of the prepared CNC, shedding against light on the contributing factors to weight loss at different temperature intervals.

Figure 7 illustrates the morphology of CNC along with the production process. In Fig. 7(a), the untreated RH fibers exhibit a smooth surface attributed to the presence of lignin, which bonded the bundles of cellulose together by ester fibers. Notably, the smooth surface indicates the cohesive properties of the untreated fibers. Upon subjecting the RH fibers to alkali treatment, as demonstrated in Fig. 7(b), there is a noticeable increase in surface roughness. This alteration in surface texture suggests a successful modification induced by the alkali treatment, potentially indicating the removal of non-cellulosic components and the enhancement of fiber structure. Figure 7(c) portrays the impact of bleaching using 2% H_2O_2 on the RH fibers. The bleaching process results in the separation of fibers into smaller bundles, and some bundles further disintegrate into individual fibers. Additionally, the fibrous diameter of the bleached RH experiences a significant reduction, approximately 96%, compared to the average untreated fibers (around 185 μm). This reduction in fiber diameter underscores the efficacy of the bleaching process in eliminating non-cellulosic components and refining the fiber structure.

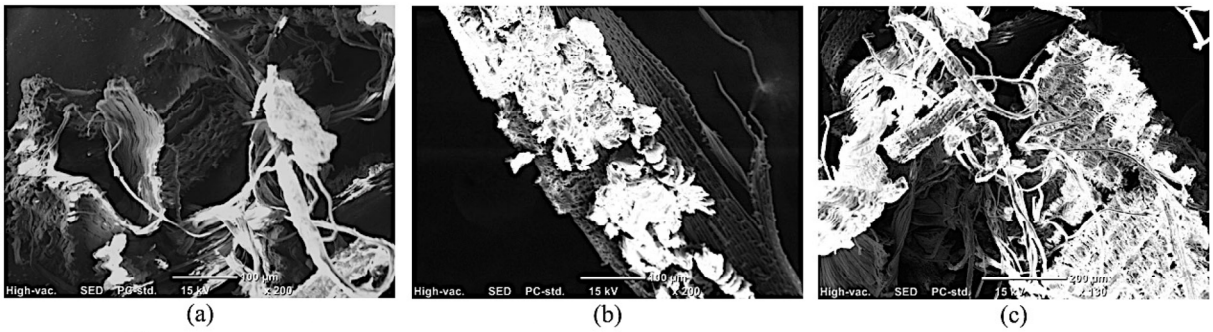

Fig. 7 SEM of the CNC during the production process at different locations. (a) The untreated RH fibers, (b) the untreated RH fibers after alkali treatment, and (c) the untreated RH fibers after the bleaching process.

The transmission electron microscope (TEM) analysis of the CNC was used to identify the dimensions of CNC, as presented in Fig. 8. The examination unveils nanoparticles characterized by a diameter spanning from 15 to 20 nm. This careful scrutiny contributes to a comprehensive comprehension of the morphological alterations within RH fibers as observed through SEM. Additionally, it delineates the nanoscale dimensions attained in the CNC via TEM, serving as a testament to the efficacy of the purification and processing methodologies applied in this study.

XRD was also utilized to identify the chemical composition of PMMA/CNC nanocomposites, as shown in Fig. 9. The PMMA sample displayed two prominent, wide XRD peaks with low intensity at 14.1° and 30.6°, showing its amorphous characteristics [39]. The presence of these peaks was likewise detected in all of the PMMA/CNC nanocomposites that were produced. The observed peaks are agreed with the outcomes studies stated by Hashem et al. [40]. The X-ray diffraction (XRD) patterns of the PMMA/CNC nanocomposites indicated an amorphous structure,

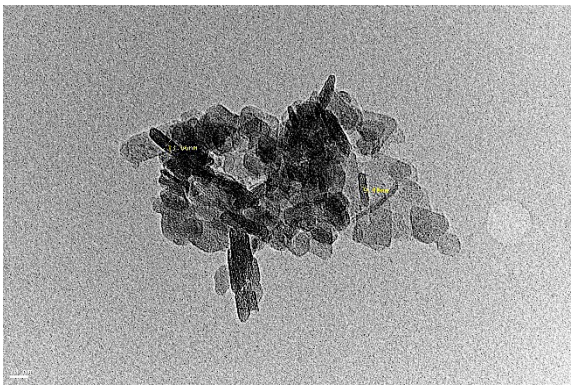

Fig. 8 TEM image of the prepared CNC.

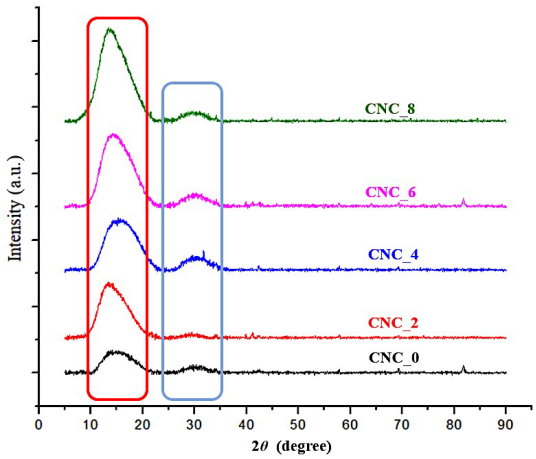

Fig. 9 XRD pattern of the prepared PMMA/CNC nanocomposites with different wt%.

suggesting that the addition of CNC did not influence the structural characteristics of PMMA and that no chemical interactions took place between CNC and PMMA.

3.2 Density and hardness of PMMA/CNC nanocomposites

The densities of the produced PMMA/CNC nanocomposites were determined as presented in Fig. 10. An incremental rise in the density of the nanocomposite was observed when the content of the added CNC increased, particularly by 5% corresponding to 0.8 wt% of CNC. The slight rise in the density is probably due to the low content of the added CNC, which did not surpass 0.8 wt%. The slight variation in the density of the nanocomposite samples ensures that lightweight PMMA remains widely applicable [41], including its utilization in dentures.

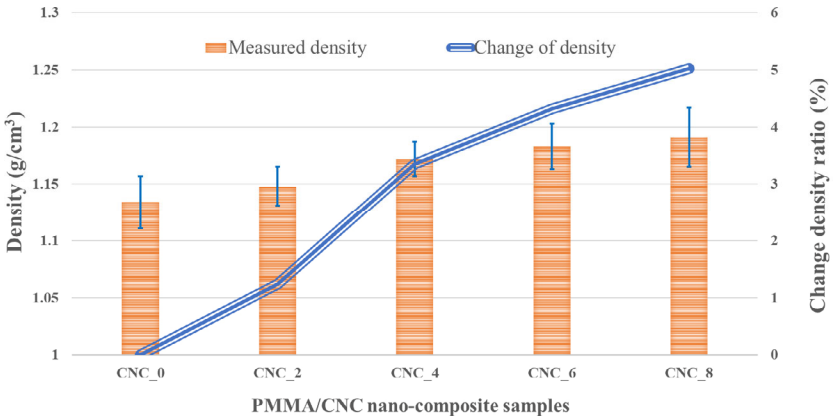

Fig. 10 Effect of the CNC addition on the density of the PMMA/CNC nanocomposites.

Figure 11 illustrates the change in nanocomposite hardness based on the change in the addition of CNC content, revealing a gradual increase with the increase of CNC weight percent. The sample CNC_8 showed the highest increasing in the hardness value of (89.7 D index), reflecting a 1.24% increase in comparison with CNC_0 (88.6 D index). The nanocomposite hardness is influenced by the intermolecular bonds strength between the CNC nanoparticles reinforced phase and the PMMA matrix phase. The observed enhancement can be attributed to the homogenous distribution of CNC nanoparticles within the PMMA [42], promoting a sufficient interface that consolidates resistance against shear stresses and improves transferring of the applied load [43]. These findings emphasize that the low CNC loading can develop the mechanical behavior of PMMA, in contrast to the higher loading of the added CNC nanoparticles which may be agglomerated in the matrix by increasing the air gaps and porosity impeded in the PMMA matrix and deteriorate the material properties [44]. It is noticed that the enhancement in the nanocomposite properties remains relatively small which could be attributed to the low weight content of CNC in the nanocomposites.

3.3 Compression strength of CNC/PMMA nanocomposites

A compression test was applied to assess the proposed PMMA/CNC nanocomposites load-carrying ability. The aim was focused on the study of the compressive properties which were achieved by adding CNC with a low content to the PMMA. The stress-strain curves were plotted during compression experiments, as shown in Fig. 12. The addition of CNC at various low content to the PMMA clearly resulted in a considerable change in the compression strength of the nanocomposites which resulted an improvement in the compressive characteristics of PMMA, when compared to pure PMMA.

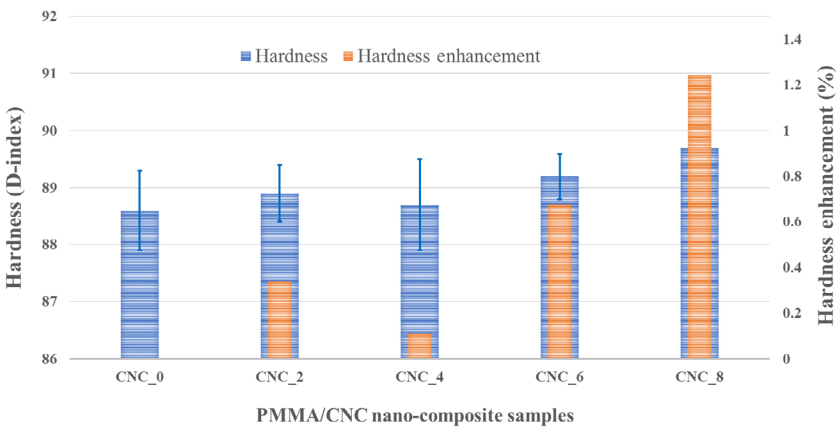

Fig. 11 Effect of the CNC wt% on the hardness values of PMMA/CNC nanocomposites.

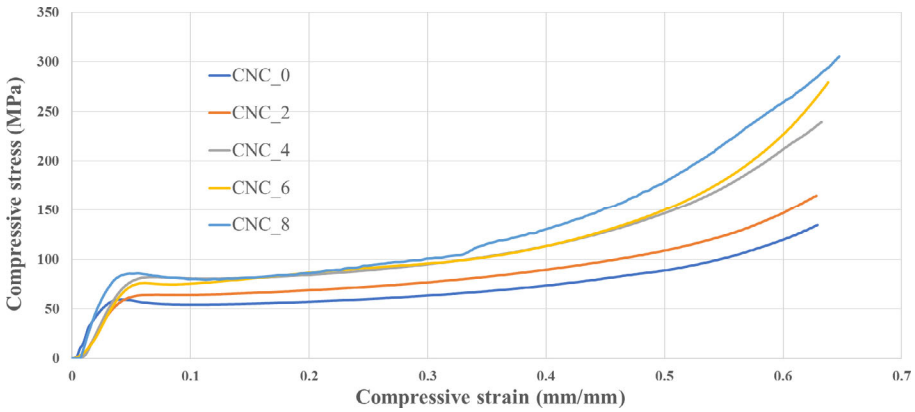

Fig. 12 Stress–strain curves of the PMMA/CNC nanocomposites with CNC wt%.

PMMA is known for its inherent brittleness and as it is commonly used as a denture foundation material, it is regularly exposed to compressive forces. Hence, it is imperative to assess the compressive characteristics of PMMA/CNC nanocomposites. Figure 13 displays the mean values of the observed yield strength and Young's modulus. It shows a clear correlation between an increase in the weight percentage of CNC and an elevation in the Young's modulus. The elastic modulus of PMMA rosed as the CNC content increased up to 0.8 wt%. The elastic modulus of CNC_4 (2.6 GPa) rose by 43.2% compared to CNC_0 (1.8 GPa). Moreover, the compressive yield strength exhibited a consistent rise when the CNC nanoparticles were loaded, resulting in a 43.24% increase for CNC_4 in comparison to CNC_0. Unlike previous research reporting the impact of incorporating a large amount of nanoparticles into PMMA, which found a decrease in compressive yield strength [45], these findings demonstrated that using a small amount of fillers can actually improve the mechanical properties. The observed rise in compressive yield strength can plausibly be ascribed to the existence of CNC nanoparticles in close proximity and evenly dispersed inside the PMMA matrix. The CNC nanoparticles possess the ability to absorb compressive loads and efficiently disperse them. Furthermore, while subjected to compression, the nanoparticles and polymer matrix aspersed the applied stress. The presence of reinforced nanoparticles in the composite material facilitated the repairing and prevented the crack propagations through the body of the sample, hence increasing its overall strength [46]. Nevertheless, it is crucial to acknowledge that this rise in strength may potentially influence the ductility of the nanocomposite material.

Figure 14 illustrates the comparative fracture toughness and ductility of the PMMA/CNC nanocomposite compressed sample. An enhancement in the ductility was observed after loading 0.8 wt% CNC nanoparticles, resulting in an increase up to 3% compared to CNC_0. Indications imply that the

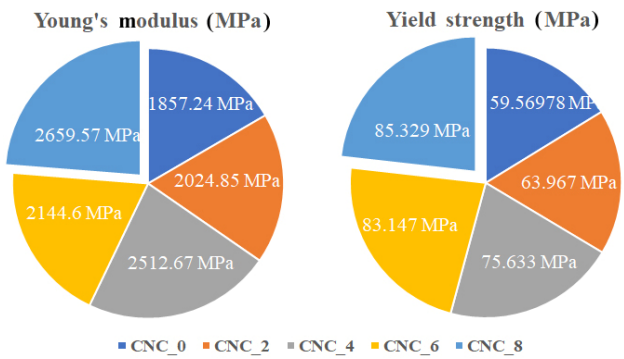

Fig. 13 Change in the Young's modulus and the yield strength of the PMMA/CNC as a function of the CNC wt%.

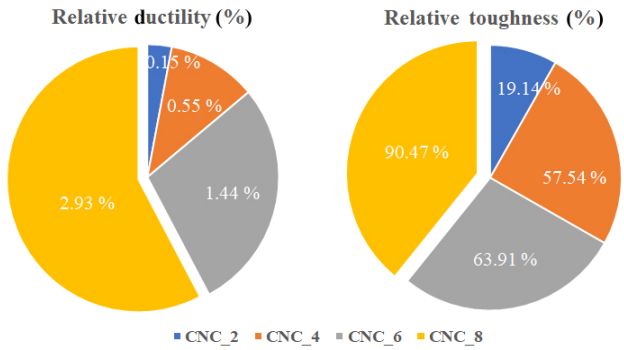

Fig. 14 Relative toughness and ductility of the PMMA/CNC as a function of the CNC wt%.

incorporating of CNC can convert the PMMA matrix from a brittle to a ductile material. The enhanced ductility might be ascribed to the energy absorption by CNC nanoparticles when subjected to compressive stresses loads, hence restricting crack propagations [47]. Additionally, the PMMA/CNC samples demonstrated better fracture toughness compared to CNC_0, possibly attributed to the inherent brittleness of the CNC_0. This suggests that CNC nanoparticles function as impact modifiers, enhancing the ability to undergo ductile fracture. Furthermore, a correlation among the CNC content and the ductility and toughness performance was observed, as these qualities are contingent upon the bonding between the PMMA matrix and the CNC reinforced nanoparticles. The enhanced toughness and ductility of the nanocomposites can be ascribed to the minimal weight percent of the CNC nanoparticles. The incorporation of substantial quantities of the added fillers nanoparticles might diminish fracture toughness by compromising the uniformity of the mixture and undermining its strength [48]. According to previous report by Chow et al. [49], the presence of excessive weight fractions can significantly reduce fracture toughness. Hence, the mechanical behavior of the PMMA matrix is considerably affected by a particular filler content.

3.4 Wear and friction properties

In order to evaluate the impact of addition of low content of CNC on the friction coefficient of PMMA/CNC nanocomposites, the produced nanocomposite specimens were tested against a stainless-steel counterpart. This rubbing was done under a range of applied loads, varying from 2 to 10 N. The sliding distances ranged from 120 to 600 m, with 0.4 m/s sliding speed. The mean friction coefficient was measured. Figure 15 displays the mean friction coefficient obtained by the friction between PMMA/CNC nanocomposites and the steel counterpart under varying normal loads and sliding distances. Generally, the coefficient of friction exhibited an elevation accompanied with the rising normal load across all composites. The CNC_6 nanocomposite recorded a 0.38 friction coefficient for a load of 2 N, which is 36.8% lower than the friction coefficient recorded

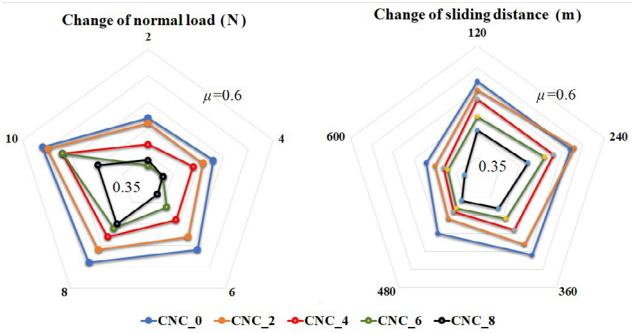

Fig. 15 Variations of PMMA/CNC nanocomposites friction coefficient with the change of normal loads and sliding distances.

when 10 N load was applied (0.52). As the normal load increases, the friction process produces more heat, which in turn causes the friction coefficient to increase. The creation of heat in this process has the effect of making the polymeric sample more pliable and causing swelling and delamination in the contact area between the surfaces that are being rubbed together [50]. The study that was carried out by Chang et al. [51], revealed that the friction coefficient increased as the temperature of the contact area during the test increased, particularly when the load increased. Additionally, CNC_8 nanocomposite exhibited the lowest friction coefficient compared with the other nanocomposites under various loadings. The friction coefficient of CNC_8 nanocomposite under a load of 6 N was measured to be 0.38, which is 34.8% lower than the friction coefficient of CNC_0 (0.51) with the same applied load of 6 N.

On the other hand, as shown in Fig. 15, it is clear that as the sliding distance increased, the friction coefficient decreased. The CNC_4 nanocomposite demonstrated a friction coefficient of 0.38 when sliding over a distance of 600 m, which is 26.3% lower than the friction coefficient observed for a sliding distance of 120 m (0.48%). This pattern for the effect of the addition of the CNC was consistent for the nanocomposites, with CNC_8 nanocomposite exhibiting the lowest coefficient of friction at various sliding distances. The reduction in the coefficient of friction can be assigned to the smoothing of the surfaces of the sample caused by extended rubbing and abrasion against the counterpart. Additionally, CNC_8 nanocomposite exhibited improved mechanical properties, specifically in terms of load-carrying capacity. This improvement in load-carrying capacity

also leads to a decrease in the friction coefficient.

In order to evaluate the extent of wear in the produced nanocomposites, the specific wear rate was investigated for both pure PMMA and PMMA/CNC nanocomposites under various loads and sliding distances. The measurements were conducted at 0.4 m/s sliding speed, and the findings are displayed in Fig. 16. The specific wear rate reduced as the content of the reinforced nanoparticles increased, indicating that this drop in the value of the wear rate may be related to the mechanical behavior of the nanocomposites. The CNC_8 nanocomposite exhibited a specific wear rate at a load of 10 N lower than CNC_0 nanocomposite by 5.22%. It is evident that the PMMA nanocomposites exhibited enhanced strength as the concentration of nanoparticles increased. Consequently, the cohesive bonds between the PMMA matrix and the CNC nanoparticles reinforcements prevented the deterioration of the nanocomposite surfaces during the friction experiment, thereby improving their ability to withstand wear. Moreover, the high wear resistance of the fabricated PMMA/CNC nanocomposites can be related to the increment in the hardness of the nanocomposite resulting from the addition of CNC nanoparticles [52]. On the contrary, an increase in the applied load substantially raised the specific wear rate. The CNC_2 nanocomposite exhibited a specific wear rate at applied load of 10 N higher than that at 2 N by 5.3%. This is mainly related to the delamination formation by the friction energy resulting from the high relative movement with the contacted surfaces. The elevated temperature had an impact on the region where the PMMA nanocomposite was in contact, causing the surface to become softer and resulting in a considerable rise in both the specific wear rate and the formation of sliding layers. Furthermore, Fig. 16 demonstrates the impact of the sliding distance on the particular wear rate of the PMMA/CNC nanocomposites. The specific wear rate is slightly reduced as the sliding distance increased. The limited impact can be ascribed to the reduction in shear resistance among the contacted surfaces caused by the transfer of PMMA layers to the counterpart.

The decrease in the coefficient of friction and specific wear rate may be due to the enhanced load-resisting ability of the produced nanocomposites by the incorporation of CNC. The load-resisting ability could be assessed by estimating the initiated stresses on the surface of the nanocomposite during the tribological test [53]. Hence, the current investigation involved building an FEM that can simulate the tribological experiment. This was accomplished by employing an ANSYS explicit dynamics package, as illustrated in Fig. 17. The stainless-steel disk has been designed in the form of a parallelogram with 120 mm in length, 30 mm in width, and 10 mm in thickness. The PMMA/CNC nanocomposite specimen was represented as a pin with 8 mm in diameter and 15 mm in height. The interaction between contact surfaces was considered to be frictional to compute the resulting stresses during the tribological test. The software tool automatically produced the corresponding meshes using hexahedron and tetrahedron shapes, resulting in a total of 1,810 nodes forms 282 elements. The PMMA/CNC nanocomposite was constrained in the x and y axes and subjected to a load of 10 N along the z-direction. The program was provided with the experimentally derived mechanical parameters of the

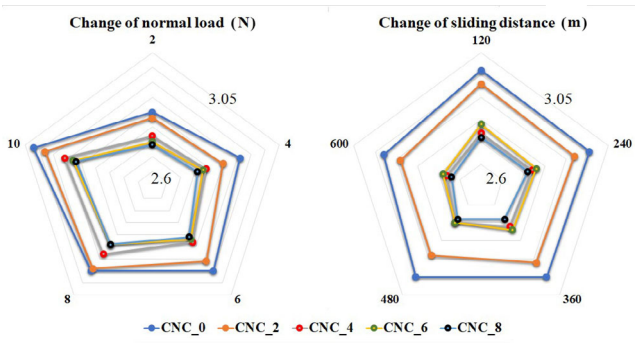

Fig. 16 Change of PMMA/CNC nanocomposites specific wear rate ($\times 10^{-3}$ mm^3/(N·m)) with the change of normal loads and sliding distances.

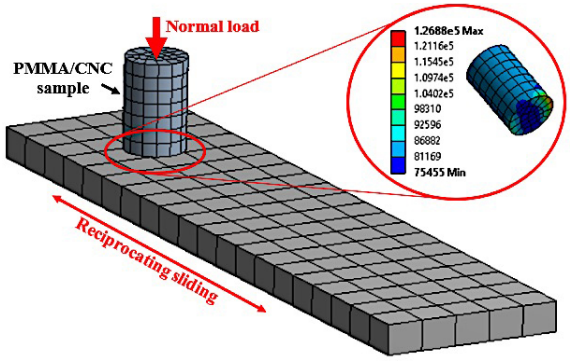

Fig. 17 FEM of the friction experiment.

various nanocomposite samples. The selected material for the counterpart was stainless steel, which moved back and forth with 0.4 m/s constant speed and had a distance of 40 mm between each movement.

Figure 17 illustrates the dispersion of contact stresses throughout the PMMA/CNC nanocomposite specimen surface. The stress localized near the periphery of the surface, most likely as a result of the direction of the friction. Figure 18 demonstrates that the inclusion of CNC resulted in a decrease in the equivalent stress on the nanocomposite surface. The observed results can be ascribed to the proven enhancement in the nanocomposites strength, resulting in a higher ability to bear loads and, consequently, a lower friction coefficient [54]. Figure 18 also shows the shear and frictional stresses produced as a function to the content of CNC nanoparticles added. The graph demonstrates a decrease in stress levels as the filler content increases, indicating a decrease in the friction coefficient [55]. Figure 16 illustrated that the wear rate throughout the rubbing experiment improved as the weight percent of CNC increased. The thickness of the worn layer was obtained using finite element analysis, as demonstrated in Fig. 18, demonstrating concurrence between simulated and practical outcomes. An increase in the CNC content caused a decrease in shear and frictional stresses on the surfaces of the sample. As a result, the thickness of the worn layer reduced, which contributed to a lower specific wear rate of the nanocomposites.

To acquire a deeper identification of the wear properties of the PMMA and PMMA/CNC nanocomposites, the surfaces of the worn samples were examined by using SEM, as shown in Fig. 19. The worn surface of CNC_0 nanocomposite displays significant wear debris and extensive peeling caused by the ploughing of its worn surface, demonstrating the deterioration of the worn surface. The degradation resulted in a significant rise in the specific wear rate, while the presence of big debris weakened the material, resulting in an increase in shear resistance and thus elevating the determined coefficient of friction [54]. In this situation, the delamination mechanism is the predominant wear mechanism. Moreover, the surface of the specimen has a rough texture, indicating a tendency for the surface to break easily and leading to a low level of toughness. The SEM analysis of the remaining composites containing cellulose nanocrystal (CNC) nanoparticles exhibited a rather smooth surface, characterized by the presence of minuscule wear debris. This demonstrates that the inclusion of CNC nanoparticles improved the strength of the surfaces of the samples, resulting in a reduction in both the specific wear rate and friction coefficient of the nanocomposite, even when the reinforced CNC nanoparticles were added in low content.

The surface of CNC_2 nanocomposite exhibits signs of damage commencement and the onset of peeling propagation. The presence of 0.2 wt% CNC led to a wear mechanism characterized by fatigue

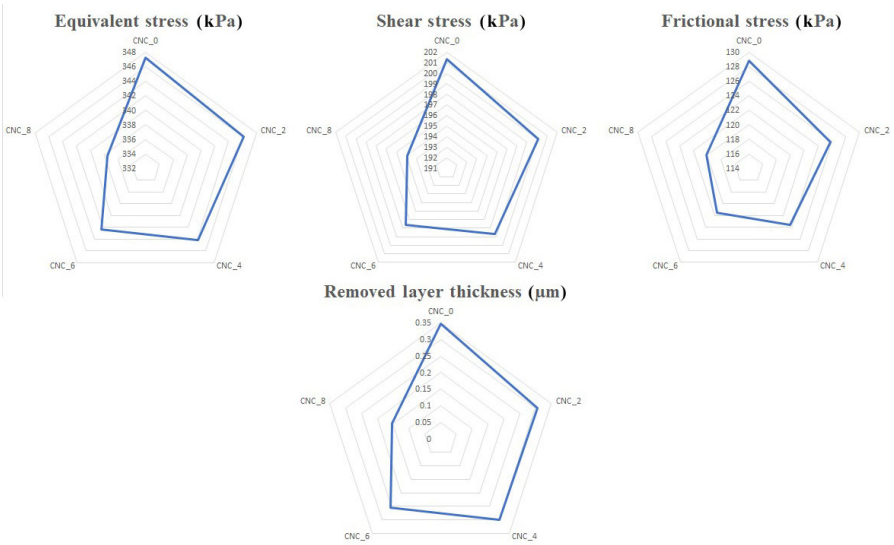

Fig. 18 Equivalent, shear, and frictional stresses generated on the PMMA/CNC samples surface and the wear layer thickness.

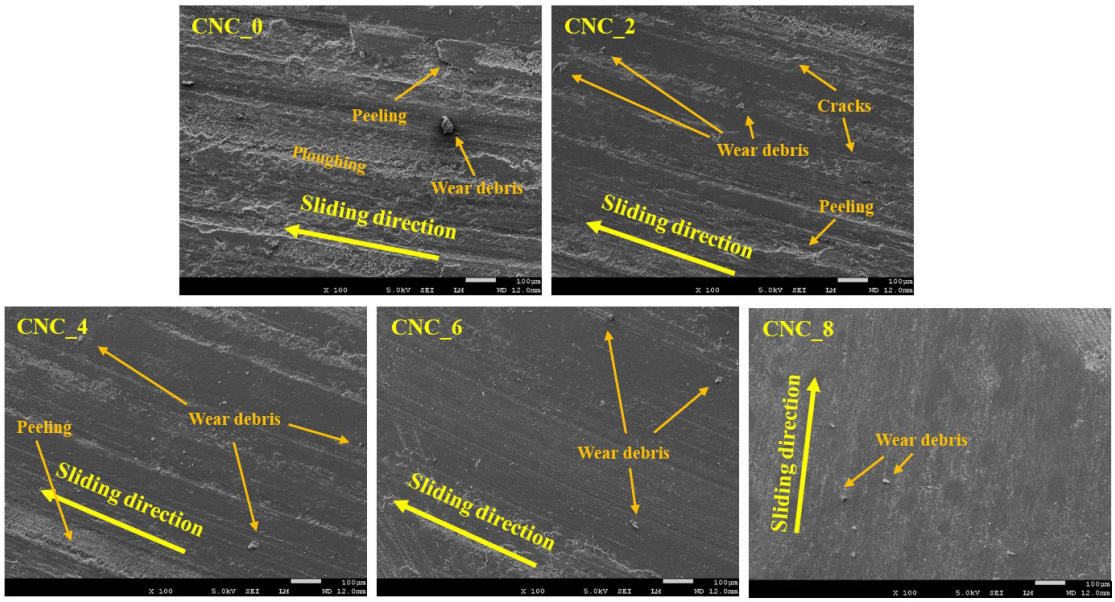

Fig. 19 SEM images of the worn surfaces of the PMMA/CNC nanocomposites.

and delamination. The addition of CNC nanoparticles at a weight percent of 0.4 wt% resulted in a partially smooth sample surface and reduced peeling, suggesting a shift in the wear mechanism towards micro-plowing. Raising the CNC content to 0.6 and 0.8 wt% resulted in an augmentation of both the bonding strength and hardness of the nanocomposite components. This led to an improvement in the interfacial adhesion among the PMMA and the CNC. This facilitated the efficient transmission of stress and enhanced the durability of the surface. Consequently, the CNC_6 and CNC_8 nanocomposites surfaces images reveal the presence of few numbers of cracks and debris on the composite surface, resulting in a decrease in the nanocomposite specimen's friction coefficient and specific wear rate.

4 Conclusions

This work examines the effects of the addition of low content of CNC nanoparticles on the PMMA, a material frequently utilized in dentures, on the mechanical and tribological characteristics of the resulting nanocomposites. Attaining a homogeneous distribution of nanoparticles within the PMMA matrix is of utmost importance, and the ball milling process was utilized to accomplish this objective. The results suggest that the incorporation of low content of nanoparticles has a negligible impact on the density of the PMMA composite, therefore maintaining its inherent lightweight characteristics. An increase in the hardness of PMMA nanocomposite by 1.2% is found, which can be attributable to the small amount of CNC added. The augmentation of CNC nanoparticle concentration from 0.2 to 0.8 wt% results in a progressive enhancement in Young's modulus and compressive yield strength by 43.2% and 43.24%, correspondingly, in comparison to pure PMMA. The fracture toughness of the 0.8 wt% PMMA nanocomposite increases by 90%. When low-loading CNC nanoparticles are added, the friction coefficient decreases by 34.8% and the wear resistance improves under different normal loads and sliding distances, as observed in tribological tests. Finite element research indicates that a small proportion of CNC in the load increases the capacity to carry the load and decreases the levels of stress and thickness of the wear layer. Analysis of worn surfaces reveals a shift in the wear mechanism and reduced wear characteristics when the weight fraction of CNC nanoparticles increases during friction.

Author contribution statement

A.F.: conceptualization, methodology, software, data curation, writing and supervision. W.M.D: data

curation, writing, supervision, project administrator, review and editing. H.I.E: conceptualization, methodology, software, data curation, and writing. H.S.A.: methodology, investigation, supervision, software, validation, review & editing.

Acknowledgements

The authors extend their appreciation to the King Salman Center for Disability Research for funding this work through Research Group (No. KSRG-2023-538).

Data availability

Data will be made available on request.

Declaration of competing interest

The authors have no competing interests to declare that are relevant to the content of this article.

References

[1] Lassila L V, Vallittu P K. Denture base polymer Alldent Sinomer: Mechanical properties, water sorption and release of residual compounds. *J Oral Rehabil* **28**(7): 607–613 (2001)

[2] Gad M M, Abualsaud R. Behavior of PMMA denture base materials containing titanium dioxide nanoparticles: A literature review. *Int J Biomater* **2019**: 6190610 (2019)

[3] Murakami N, Wakabayashi N, Matsushima R, Kishida A, Igarashi Y. Effect of high-pressure polymerization on mechanical properties of PMMA denture base resin. *J Mech Behav Biomed Mater* **20**: 98–104 (2013)

[4] Alhareb A O, Akil H M, Ahmad Z A. Mechanical properties of PMMA denture base reinforced by nitrile rubber particles with Al_2O_3/YSZ fillers. *Procedia Manuf* **2**: 301–306 (2015)

[5] Darbar U R, Huggett R, Harrison A. Denture fracture: A survey. *Br Dent J* **176**(9): 342–345 (1994)

[6] Fouly A, Taha M, Albahkali T, Ali Shar M, Abdo H S, Nabhan A. Developing artificial intelligence models for predicting the tribo-mechanical properties of HDPE nanocomposite used in artificial hip joints. *IEEE Access* **12**: 14787–14799 (2024)

[7] Li R Z, Ye L, Mai Y W. Application of plasma technologies in fibre-reinforced polymer composites: A review of recent developments. *Compos Part A Appl Sci Manuf* **28**(1): 73–86 (1997)

[8] Paul A, Kesharvani S, Agrawal A, Dwivedi G, Singh V, Saxena K K. Mechanical and tribological properties of nano clay/PMMA composites extruded with a twin-screw extruder. *P I Mech Eng E-J Pro* https://doi.org/10.1177/0954408923121522 (2023)

[9] Kanie T, Fujii K, Arikawa H, Inoue K. Flexural properties and impact strength of denture base polymer reinforced with woven glass fibers. *Dent Mater* **16**(2): 150–158 (2000)

[10] Asar N V, Albayrak H, Korkmaz T, Turkyilmaz I. Influence of various metal oxides on mechanical and physical properties of heat-cured polymethyl methacrylate denture base resins. *J Adv Prosthodont* **5**(3): 241 (2013)

[11] Alhareb A O, Ahmad Z A. Effect of Al_2O_3/ZrO_2 reinforcement on the mechanical properties of PMMA denture base. *J Reinf Plast Compos* **30**(1): 86–93 (2011)

[12] Alhareb A O, Akil H M, Ahmad Z A. Impact strength, fracture toughness and hardness improvement of PMMA denture base through addition of nitrile rubber/ceramic fillers. *Saudi J Dent Res* **8**(1–2): 26–34 (2017)

[13] Fouly A, Ibrahim A M M, El-Bab A M. Promoting the tribological properties of epoxy composites via using graphene nanoplatelets as a functional additive. *KGK-Kautsch Gummi Kunststoffe* **73**: 25–32 (2020)

[14] Badran A H, Alamro T, Bazuhair R W, Ali Gad El-Mawla A, El-Adben S Z, Fouly A. Investigation of the mechanical behavior of synthesized Al6061/TiO_2 microcomposites using an innovative stir casting method. *Nanomaterials* **12**(10): 1646 (2022)

[15] Jordan J, Jacob K I, Tannenbaum R, Sharaf M A, Jasiuk I. Experimental trends in polymer nanocomposites—A review. *Mater Sci Eng A* **393**(1–2): 1–11 (2005)

[16] Shakeri F, Nodehi A, Atai M. PMMA/double-modified organoclay nanocomposites as fillers for denture base materials with improved mechanical properties. *J Mech Behav Biomed Mater* **90**: 11–19 (2019)

[17] Salahuddin N, El-Kemary M, Ibrahim E. Reinforcement of polymethyl methacrylate denture base resin with ZnO nanostructures. *Int J Appl Ceram Technol* **15**(2): 448–459 (2018)

[18] Salim F M. Tribological and mechanical characteristics of dental fillings nanocomposites. *Energy Procedia* **157**: 512–521 (2019)

[19] Rashed A, Nabhan A. Influence of adding nano graphene and hybrid SiO_2-TiO_2 nano particles on tribological characteristics of polymethyl methacrylate (PMMA). *KGK-Kautsch Gummi Kunststoffe* **71**: 32–37 (2018)

[20] Yang Z, Dong B, Huang Y, Liu L, Yan F Y, Li H L. A study on carbon nanotubes reinforced poly(methyl methacrylate) nanocomposites. *Mater Lett* **59**(17): 2128–2132 (2005)

[21] Farhan F K, Kadhim B B, Ablawa B D, Shakir W A. Wear and friction characteristics of TiO_2–ZnO/PMMA nanocomposites. *Eur J Eng Technol Res* **2**(4): 6–9 (2017)

[22] Ameer A K, Mousa M O, Ali W Y. Tribological behaviour of poly-methyl methacrylate reinforced by multi-walled carbon nanotubes. *KGK-Kautsch. Gummi Kunststoffe* **71**: 40–46 (2018)

[23] Taha M, Fouly A, Abdo H S, Alnaser I A, Abouzeid R, Nabhan A. Unveiling the potential of rice straw nanofiber-reinforced HDPE for biomedical applications: Investigating mechanical and tribological characteristics. *J Funct Biomater* **14**(7): 366 (2023)

[24] Mariano M, El Kissi N, Dufresne A. Cellulose nanocrystals and related nanocomposites: Review of some properties and challenges. *J Polym Sci B Polym Phys* **52**(12): 791–806 (2014)

[25] Iwamoto S, Kai W H, Isogai A, Iwata T. Elastic modulus of single cellulose microfibrils from tunicate measured by atomic force microscopy. *Biomacromolecules* **10**(9): 2571–2576 (2009)

[26] Kausch H H, Michler G H. Effect of nanoparticle size and size-distribution on mechanical behavior of filled amorphous thermoplastic polymers. *J Appl Polym Sci* **105**(5): 2577–2587 (2007)

[27] Oksman K, Mathew A P, Bondeson D, Kvien I. Manufacturing process of cellulose whiskers/polylactic acid nanocomposites. *Compos Sci Technol* **66**(15): 2776–2784 (2006)

[28] Fouly A, Albahkali T, Ali Shar M, Abdo H S, Taha M. Casting light on the tribological properties of paraffin-based HDPE enriched with graphene nano-additives: An experimental investigation. *Mater Res Express* **10**(12): 125301 (2023)

[29] Talari F, Qujeq D, Amirian K, Ramezani A, Pourkhalili H, Alhavaz A. Evaluation the effect of cellulose nanocrystalline particles on flexural strength and surface hardness of autoploymerized temporary fixed restoration resin. *Int J Adv Biotechnol Res* **7**: 152–160 (2016)

[30] Sabir M, Ali A, Siddiqui U, Muhammad N, Khan A S, Sharif F, Iqbal F, Shah A T, Rahim A, Rehman I U. Synthesis and characterization of cellulose/hydroxyapatite based dental restorative composites. *J Biomater Sci Polym Ed* **31**(14): 1806–1819 (2020)

[31] Fouly A, Ibrahim A M M, Sherif E M, FathEl-Bab A M R, Badran A H. Effect of low hydroxyapatite loading fraction on the mechanical and tribological characteristics of poly(methyl methacrylate) nanocomposites for dentures. *Polymers* **13**(6): 857 (2021)

[32] Mohazzab P. Archimedes' principle revisited. *J Appl Math Phys* **5**(4): 836–843 (2017)

[33] ISO 14126:2023. Fibre-reinforced plastic composites—Determination of compressive properties in the in-plane direction. ISO, 1999.

[34] Zhao H, Allanson D, Ren X J. Use of shore hardness tests for In-process properties estimation/monitoring of silicone rubbers. *J Mater Sci Chem Eng* **3**(7): 142–147 (2015)

[35] US-ASTM. ASTM G 99–04 Standard test method for wear testing with a pin-on-disk apparatus. ASTM, 2008.

[36] Ünalan F, Gürbüz Ö, Nihan N, Bilgin P, Sermet B. Effect of mica as filler on wear of denture teeth polymethylmethacrylate (PMMA) resin. *Balk J Stomatol* **11**: 133–137 (2007)

[37] Champagne C, Waggoner W, Ditmyer M, Casamassimo P S, MacLean J. Parental satisfaction with preveneered stainless steel crowns for primary anterior teeth. *Pediatr Dent* **29**(6): 465–469 (2007)

[38] Fathi H I, El-Shazly A H, Elkady M F, Madih K. Assessment of new technique for production cellulose nanocrystals from agricultural waste. *Mater Sci Forum* **928**: 83–88 (2018)

[39] Rameshkumar C, Sarojini S, Naresh K, Subalakshmi R. Preparation and characterization of pristine PMMA and PVDF thin film using solution casting process for optoelectronic devices. *J Surf Sci Technol* **33**(1–2): 12 (2017)

[40] Hashem M, Rez M F, Fouad H, Elsarnagawy T, Elsharawy M, Umar A, Assery M, Ansari S G. Influence of titanium oxide nanoparticles on the physical and thermomechanical behavior of poly methyl methacrylate (PMMA): A denture base resin. *Sci Adv Mater* **9**(6): 938–944 (2017)

[41] Ramanathan T, Stankovich S, Dikin D A, Liu H, Shen H, Nguyen S T, Brinson L C. Graphitic nanofillers in PMMA

nanocomposites—An investigation of particle size and dispersion and their influence on nanocomposite properties. *J Polym Sci B Polym Phys* **45**(15): 2097–2112 (2007)

[42] Karthick R, Sirisha P, Sankar M R. Mechanical and Tribological Properties of PMMA-Sea Shell based Biocomposite for Dental application. *Procedia Mater Sci* **6**: 1989–2000 (2014)

[43] Elmadani A A, Radović I, Tomić N Z, Petrović M, Stojanović D B, Heinemann R J, Radojević V. Hybrid denture acrylic composites with nanozirconia and electrospun polystyrene fibers. *PLoS One* **14**(12): e0226528 (2019)

[44] Ananthu M, Shamnadh M, Dileep P N. Experimental evaluation on mechanical properties and wear resistance in PMMA seashell bionanocomposite for medical application. *Mater Today Proc* **5**(11): 25657–25666 (2018)

[45] Zebarjad S M, Sajjadi S A, Sdrabadi T E, Sajjadi S A, Yaghmaei A, Naderi B. A study on mechanical properties of PMMA/hydroxyapatite nanocomposite. *Engineering* **3**(8): 795–801 (2011)

[46] Yang K, Ritchie R O, Gu Y Z, Wu S J, Guan J. High volume-fraction silk fabric reinforcements can improve the key mechanical properties of epoxy resin composites. *Mater Des* **108**: 470–478 (2016)

[47] Franklin P, Wood D J, Bubb N L. Reinforcement of poly(methyl methacrylate) denture base with glass flake. *Dent Mater* **21**(4): 365–370 (2005)

[48] Rajkumar K, Sirisha P, Sankar M R. Tribomechanical and surface topographical investigations of poly methyl methacrylate-seashell particle based biocomposite. *Procedia Mater Sci* **5**: 1248–1257 (2014)

[49] Chow W S, Tay H K, Azlan A, Ishak Z M. Mechanical and thermal properties of hydroxyapatite filled poly (methyl methacrylate) composites. In *Proceedings of the Proceedings of the Polymer Processing Society 24th Annual Meeti*ng, 2008.

[50] Khun N W, Zhang H, Lim L H, Yue C Y, Hu X, Yang J L. Tribological properties of short carbon fibers reinforced epoxy composites. *Friction* **2**(3): 226–239 (2014)

[51] Chang L, Zhang Z, Zhang H, Friedrich K. Effect of nanoparticles on the tribological behaviour of short carbon fibre reinforced poly(etherimide) composites. *Tribol Int* **38**(11–12): 966–973 (2005)

[52] Campos-Sanabria V, Hernández-Sierra M T, Bravo-Sánchez M G, Aguilera-Camacho L D, García-Miranda J S, Moreno K J. Tribological and mechanical characterization of PMMA/HAp nanocomposites obtained by free-radical polymerization. *MRS Adv* **3**(63): 3763–3768 (2018)

[53] Kuminek T, Aniołek K, Młyńczak J. A numerical analysis of the contact stress distribution and physical modelling of abrasive wear in the tram wheel-frog system. *Wear* **328–329**: 177–185 (2015)

[54] Tang W, Zhou Y K, Zhu H, Yang H F. The effect of surface texturing on reducing the friction and wear of steel under lubricated sliding contact. *Appl Surf Sci* **273**: 199–204 (2013)

[55] Fouly A, Alkalla M G. Effect of low nanosized alumina loading fraction on the physicomechanical and tribological behavior of epoxy. *Tribol Int* **152**: 106550 (2020)

Ahmed FOULY. He received his B.S. degree in mechanical engineering from Minia University, Minia, Egypt, with grade distinction with honor's degree in 2009. He received his M.S. degree in mechanical engineering from the same university in 2013. He received his Ph.D. degree in mechatronics and robotics engineering from the School of Innovative Design Engineering, Egypt-Japan University of Science and Technology, Egypt, in 2017. He is now an associate professor at Mechanical Engineering Department, College of Engineering, King Saud University. His current interests include material science, tribology, composite materials, contact physics, micro tactile sensors, and micro fabrication.